Int. j. adv. multidisc. res. stud. 2023; 3(4):44-53

Received: 14-05-2023
Accepted: 24-06-2023

International Journal of Advanced Multidisciplinary Research and Studies

ISSN: 2583-049X

Effect of Heat Generation and Magneto-Hydrodynamics on Unsteady Casson Non-Newtonian Hybrid Nanofluid Flow over a Stretching Porous Medium

[1] Victor Olajide Akinsola, [2] Akintayo Oladimeji Akindele, [3] Adekunle Aworinde, [4] Moses Olayemi Adeyemi, [5] Olusegun Adebayo Ajala, [6] Musilim Taiwo

[1] Department of Mathematics, Adeleke University Ede, Osun State, Nigeria
[2, 3, 4, 5] Department of Pure and Applied Mathematics, Ladoke Akintola University of Technology, Ogbomoso, Nigeria
[6] Department of Mathematics, Osun State College of Education, Ila-Orangun, Osun State, Nigeria

Corresponding Author: **Akintayo Oladimeji Akindele**

Abstract
The research numerically analyzed the effect of heat generation and magneto-hydrodynamics (MHD) on unsteady Casson non-Newtonian hybrid nanofluid flow over a stretching porous medium. Further effects involved in the main model are vertically applied magnetic flux, and viscous dissipation effect. The Finite Difference method (FDM) was used to solve the ordinary differential equations (ODEs) with MAPLE 18.0 software. The results were visualized using tables and graph to illustrate the effects of fluid physical quantities, fluid momentum, energy distribution, hybrid nanoparticles concentration, and velocity profiles for various applicable values of dimensionless numbers. The numerical outcomes of the effects of different physical parameters of the fluid were demonstrated and it was noticed that velocity profile increased as the thermal Grashof numbers increased as a result of an increase in buoyant force caused by convent heat generation through the upper plate of the fluid and reduced as Casson fluid parameter increased because of decrease in magnetic and heat dissipation parameters. The research work is economically valuable for mechanical engineers, physicists, chemists, marine engineers, and other fields since its applications brings about their operational improvement.

Keywords: Casson Fluid, Heat Generation, Magneto-Hydrodynamics, Thermal Grashof Numbers, Stretching Porous Medium

1. Introduction

The rheology of Casson non-Newtonian flow in the porous media has become major academic research topics over the years because of its significant in natural sciences, engineering, and pharmaceutical fields. It is imperative to study behavior of the Casson non-Newtonian hybrid nanofluids flow in order to have detail understanding of these fluids and their different applications. Heat performance of energy change systems is one of the most crucial objectives to improve the efficiency of systems. Such heat performance is mainly dependent on the thermo-physical properties of the fluids used in the systems energy change. The properties include thermal and electrical conductivities, isochoric specific heat change, and dynamics viscosity. These properties altered the thermal transfer capacity features of the fluids. The recent developments in engineering field are raising the needs of excellent compact devices with best performance, perfect operation and prolonged life span. The hybrid nanoparticles enhance its thermal conductivity in different heat applications such as automobile manufacturing processes, HVAC and solar panels. Moreover, in order to meet high power density necessities in modern high-heat-flux devices, efficient heat transfer processes play a support role. Rashidi *et al.* [1] worked on the heat performance of energy changing systems, which is one of the most crucial objectives to improve the efficiency of systems. Such heat performance is mainly dependent on the thermo-physical properties of the fluids used in the systems energy change. Rehman *et al.* [2] approximate analytical analysis of unsteady MHD mixed flow of non-newtonian hybrid nanofluid over a stretching surface. Zaimi *et al.* [3] examined boundary layer flow and heat transfer past a permeable shrinking sheet in a nanofluid with radiation effect.

Kamran *et al.* [4] numerically investigate Casson nanofluid flow with joule heating and slip effect. Ogunsola and Akindele [5] analyze the mixture of Al_2O_3-Cu/H_2O-$(CH_2OH)_2$ MHD hybrid nanofluid flow due to a stretchable rotating disks system under the influence of non-uniform heat source or sink and thermal radiation. Makinde and Aziz [6] considered the boundary layer flow of a nanofluid past a stretching sheet with a convective boundary. Ghadikolaei *et al.* [7] study the properties of TiO2-Cu/H2O a hybrid nanofluid in the presence of resistance force. Omar *et al.* [8] observed stagnation point flow over a stretching or shrinking Cylinder in a Copper-Water Nanofluid. Tayebi and Chamkha [9] studied the free convection enhancement in an

annulus between horizontal confocal elliptical cylinders using hybrid nanofluids. Kamel *et al.* [10] experimentally studied thermal conductivity of Al_2 O_3 and CeO_2 nanoparticles and their hybrid-based water nanofluids. Lund *et al.* [11] carried out triple solutions and stability analysis on MHD flow of micro-polar fluid with effects of viscous dissipation and joule. Mjankwi [12] studied unsteady MHD Flow of Nanofluid with Variable Properties over a Stretching Sheet in the Presence of Thermal Radiation and Chemical Reaction. Sobamowo *et al.* [13] offered thermos magneto-solutal squeezing flow of nanofluid sandwiched between two parallel disks inserted in a porous medium and give account of the effects of nanoparticles geometry slip and temperature jump conditions. Waini *et al.* [14] studied the unsteady Casson fluid flow and heat transfer over a stretching surface with modified magnetic field effects. Goud *et al.* [15] analyze the radiation effect on MHD Casson fluid flow over an inclined non-linear surface with chemical reaction in a Forchheimer porous medium. Mukhopadhyay *et al.* [16] considered the effect of Casson fluid flow over unsteady stretching surface.Some recent studies on nanofluid flows are mentioned in the references [17-23].

The objective of this research is to examine the effect of heat generation and MHD on unsteady Casson non-Newtonian hybrid nanofluid flow over-stretching porous medium. The unsteadiness, velocity, thermal and magnetic fields were given attention. The systems of governing non-linear partial differential equations were reformed into their ordinary differential equation equivalents and the resulting equations were solved numerically by MAPLE 18.0 software with FDM subjected to suitable boundary conditions.

2. Methodology

2.1 Model Formulations

The equations that control the isotropic, as well as incompressible Casson flow are as follows:

$$\tau_{ij} = \begin{cases} 2\left(\mu_B + \frac{P_y}{\sqrt{2\pi}}\right)e_{ij}, & \pi > \pi_c \\ 2\left(\mu_B + \frac{P_y}{\sqrt{2\pi_c}}\right)e_{ij}, & \pi < \pi_c \end{cases}$$

Where, τ_{ij}, μ_B, P_y, $\pi = e_{ij}e_{ij}$, $e_{ij} = (i, j)th$, π_c are respectively the Stress tensor, Non-Newtonian fluid dynamic viscosity, Fluid yield stress of the liquid, product of the rate of strain tensor with tensor, component of the deformation rate, the critical value of the product based on the non-Newtonian model.

Consider a completely developed two-dimensional, viscous, unsteady, MHD and non-Newtonian Casson hybrid nanofluid flow with vertically applied magnetic in the presence of convective heat generation and electrical conductivity in a stretching Forchheimer porous media as shown Fig 1 geometrically. The cavity enclosed a fluid that is considered as a hybrid nanofluid with basefluid as a mixture of ethylene glycol ($C_2H_6O_2$) and water (H_2O) in a ratio 50:50.The governing equations of continuity, momentum and energy are written as below with the boundary layer approximations.

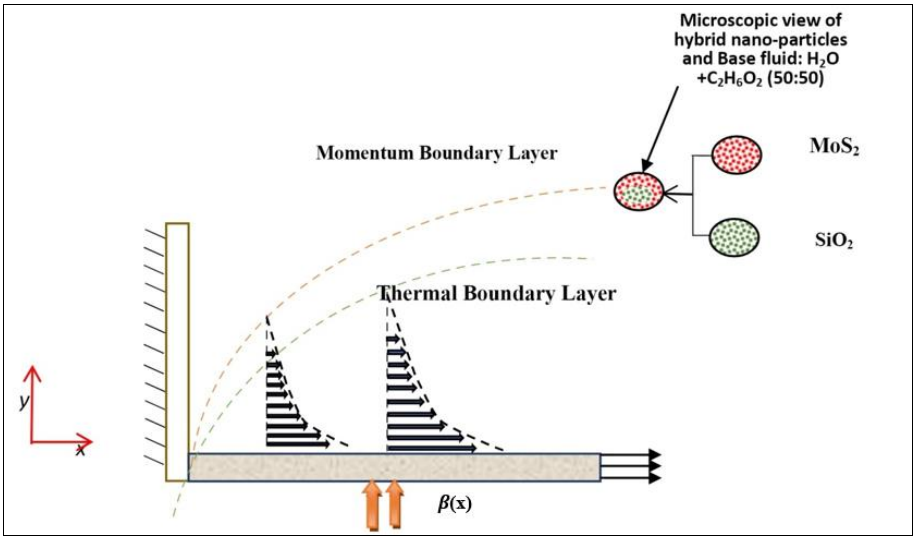

Fig 1: Physical model of the coordinate system

$$\frac{\partial u}{\partial x} + \frac{\partial u}{\partial y} = 0 \tag{1}$$

$$\frac{\partial u}{\partial t} + u\frac{\partial u}{\partial y} + v\frac{\partial u}{\partial y} = v_{hnf}\left(1 + \frac{1}{\beta}\right)\frac{\partial^2 u}{\partial y^2} + g\beta_T(T - T_\infty) - \frac{\sigma_{hnf}B^2(x,t)}{\rho_{hnf}}u - \frac{v_{hnf}}{k}u - \frac{b}{k}u^2 \tag{2}$$

$$\frac{\partial T}{\partial t} + u\frac{\partial T}{\partial x} + v\frac{\partial T}{\partial y} = \frac{k_{hnf}}{(\rho c_p)_{hnf}}\frac{\partial^2 T}{\partial y^2} + \frac{Q_0(T - T_\infty)}{(\rho c_p)_{hnf}} + \frac{v_{hnf}}{c_p}\left(\frac{\partial u}{\partial y}\right)^2 + \frac{\sigma_{hnf}B^2(x,t)}{(\rho c_p)_{hnf}}u^2 \tag{3}$$

The boundary conditions for the models are given by:

$$\begin{cases} u = u_w(x,t), v = v_w, T = T_\infty(x,t) asy = 0 \\ u \to 0, T \to T_\infty asy \to 0 \end{cases} \quad (4)$$

The stream functions is define as

$$u = \frac{\partial \psi}{\partial y} \quad and \quad v = -\frac{\partial \psi}{\partial x}$$

The similarity incorporated as

$$\eta = y\sqrt{\frac{c}{\nu(1-\alpha t)}}, \psi = \sqrt{\frac{c\nu}{(1-\alpha t)}} x f(\eta), \theta(\eta) = \frac{T-T_\infty}{T_w - T_\infty}, B^2(x,t) = B_0{}^2(1-\alpha t)^{-1} \} \quad (5)$$

Table 1: Thermo- physical properties of hybrid base fluid and nanoparticles

Physical Properties	$C_2H_6O_2$	MoS_2	SiO_2
$\rho\left(\frac{kg}{m^3}\right)$	1113.5	2650	5060
$C_p\left(\frac{J}{kg \cdot k}\right)$	2430	730	397.746
$k\left(\frac{W}{m \cdot k}\right)$	0.253	1.5	34.5

Table 2: Thermo-Physical properties comparison between nanofluid and hybrid nanofluid

Properties	Nanofluid	Hybrid Nanofluid
Viscosity	$\mu_{nf} = \frac{\mu_f}{(1-\varphi)^{2.5}}$	$\mu_{hnf} = \frac{\mu_f}{(1-\varphi_1)^{2.5}(1-\varphi_2)^{2.5}}$
Density	$\rho_{nf} = \rho_f\left(1-\varphi+\varphi\left(\frac{\rho_s}{\rho_f}\right)\right)$	$\rho_{hnf} = \rho_f(1-\varphi_2)\left(1-\varphi_1+\varphi_1\left(\frac{\rho_{s1}}{\rho_f}\right)\right)+\varphi_2\rho_{s2}$
Electric Conductivity	$\sigma_{nf} = \sigma_f\left(1+\frac{3\left(\frac{\sigma_s}{\sigma_f}-1\right)\varphi}{2+\frac{\sigma_s}{\sigma_f}-\left(\frac{\sigma_s}{\sigma_f}-1\right)\varphi}\right)$	$\frac{\sigma_{hnf}}{\sigma_f} = 1+\frac{3\varphi(\varphi_1\sigma_1+\varphi_2\sigma_2-\sigma_{bf}\varphi)}{\varphi_1\sigma_1+\varphi_2\sigma_2+2\varphi\sigma_{bf}-\varphi\sigma_{bf}(\varphi_1\sigma_1+\varphi_2\sigma_2-\sigma_{bf}\varphi)}$ $\varphi = (\varphi_1+\varphi_2)$
Coefficient of thermal expansion	$(\rho\beta)_{nf} = (\rho\beta)_f\left(1-\varphi+\varphi\frac{(\rho\beta)_s}{(\rho\beta)_f}\right)$	$(\rho\beta)_{hnf} = (\rho\beta)_f(1-\varphi_2)\left(1-\varphi_1+\varphi_1\frac{(\rho\beta)_{s1}}{(\rho\beta)_f}\right)+\varphi_2(\rho\beta)_{s2}$
Heat Capacity	$(\rho Cp)_{nf} = (\rho Cp)_f\left(1-\varphi+\varphi\frac{(\rho Cp)_s}{(\rho Cp)_f}\right)$	$(\rho Cp)_{hnf} = (\rho Cp)_f(1-\varphi_2)\left(1-\varphi_1+\varphi_1\frac{(\rho Cp)_{s1}}{(\rho Cp)_f}\right)$ $+\varphi_2(\rho Cp)_{s2}$
Thermal Conductivity	$\frac{k_{nf}}{k_f} = \frac{k_s+(m-1)k_f-(m-1)\varphi(k_f-k_s)}{k_s+(m-1)k_f+\varphi(k_f-k_s)}$	$\frac{k_{hnf}}{k_{bf}} = \frac{k_{s2}+(m-1)k_{bf}-(m-1)\varphi_2(k_{bf}-k_{s2})}{k_{s2}+(m-1)k_{bf}+\varphi_2(k_{bf}-k_{s2})}$ *where* $\frac{k_{bf}}{k_f} = \frac{k_{s1}+(m-1)k_f-(m-1)\varphi_1(k_f-k_{s1})}{k_{s1}+(m-1)k_f+\varphi_1(k_f-k_{s1})}$

Equation (1) is identically satisfied, substituting (5) into(2) and(3) yields

$$\frac{1}{\varepsilon_1}\left(1+\frac{1}{\beta}\right)f''' + ff'' + Gr\theta - A\left(f' + \frac{\eta}{2}f''\right) - \left(\frac{\varepsilon_2}{\varepsilon_3}M + f'\right)f' - \frac{Re\,x}{\varepsilon_1 Da}f' - Fs(f')^2 = 0 \quad (6)$$

$$\frac{\varepsilon_5}{\varepsilon_4}\frac{1}{\Pr}\theta'' + \frac{1}{\varepsilon_1}Ec(f'')^2 + f\theta' + \frac{\varepsilon_2}{\varepsilon_4}EcM(f')^2 + \frac{1}{\varepsilon_4}Q\theta - \frac{A\eta}{2}\theta' = 0 \quad (7)$$

The derivative with regard to η is denoted by the prime that goes with each profile and the boundary

$$\begin{cases} f = fw, f' = 1, \theta = 1 \\ f'(\eta) \to 1, \theta(\eta) \to 0 as \eta \to \infty \end{cases} \quad (8)$$

Where

$$\varepsilon_1 = (1-\varphi_1)^{2.5}(1-\varphi_2)^{2.5}(1-\varphi_2)\left(1-\varphi_1+\varphi_2\left(\frac{\rho_{s1}}{\rho_f}\right)\right)+\varphi_2\rho_{s2}$$

$$\varepsilon_2 = 1+\frac{3(\phi_1+\phi_2)\left(\phi_1\sigma_1+\phi_2\sigma_2-\sigma_{bf}(\phi_1+\phi_2)\right)}{\phi_1\sigma_1+\phi_2\sigma_2+2(\phi_1+\phi_2)\sigma_{bf}-(\phi_1+\phi_2)\sigma_{bf}\left(\phi_1\sigma_1+\phi_2\sigma_2-\sigma_{bf}(\phi_1+\phi_2)\right)}$$

$$\varepsilon_3 = \rho_f(1-\phi_2)\left(1-\phi_1+\phi_1\left(\frac{\rho_{s1}}{\rho_f}\right)\right)+\phi_2\rho_{s2}$$

$$\varepsilon_4 = (\rho Cp)_f(1-\varphi_2)\left(1-\varphi_1+\varphi_1\frac{(\rho Cp)_{s1}}{(\rho Cp)_f}\right)+\varphi_2(\rho Cp)_{s2}$$

$$\varepsilon_5 = \left(\frac{k_{s1}+(m-1)k_f-(m-1)\phi_1(k_f-k_{s1})}{k_{s1}+(m-1)k_f+\phi_1(k_f-k_{s1})}\right)\times\left(\frac{k_{s2}+(m-1)k_{bf}-(m-1)\phi_2(k_{bf}-k_{s2})}{k_{s2}+(m-1)k_{bf}+\phi_2(k_{bf}-k_{s2})}\right)$$

$$\boldsymbol{A=\frac{\alpha}{c}, M=\frac{\sigma_f}{\rho_f c}B_0{}^2, Fs=\frac{bx}{k^*}, Da=\frac{k'}{x^2}, Re\,x=\frac{cx^2}{(1-\alpha t)\nu_f}, Gr=\frac{(1-\alpha t)^2 g\beta_T(T_w-T_\theta)}{c^2 x}\ Pr=\frac{(\rho c_p)_f\nu}{k_f}, Ec=\frac{c^2x^2}{c_p(T_w-T_\infty)(1-\alpha t)^2}, Q=\frac{(1-\alpha t)Q_0}{c(\rho c_p)_f}}$$

Unsteadiness Parameter, Magnetic Parameter, Forchheimer, Darcy, Reynold number, Thermal GrashofPrandtl, Eckert number, and Heat Source Parameter.

The parameters of significant interest for the present problem are the skin-friction coefficient C_f and local Nusselt number Nuwhich are given by:

$$C_f = \frac{\tau_w}{\rho_{hnf}u_w}, Nu = \frac{xq_w}{k_f(T_w-T_\infty)}$$

Using the similarity variables

$$C_f Re_x^{1/2} = \frac{1}{(1-\phi_1)^{2.5}(1-\phi_2)^{2.5}}\left(1+\frac{1}{\beta}\right)f''(0)$$

$$Nu\,Re_x^{1/2} = -\frac{k_{hnf}}{k_f}\theta'(0)$$

2.2 Numerical Computational

The Finite Difference Method was employed to solve equations (6) and (7) together with boundary conditions (8) numerically with the aid of Mable 18.0 software which comprises the following itemization:

1. The reduction of non-linear ordinary differential equations into first order system
2. Finite Different Discretization
3. Using Newton's Method for Linearization

3. Results and Discussion

This specific study is to develop a perfect understanding of the effect of heat generation and magnetic field on unsteady Casson non-Newtonian flow over stretching porous medium, the velocity, heat generation and porous medium heat gradient solution are presented numerically. Fig 2 indicates the effect of the unsteadiness parameter on the fluid velocity profile. It is noted that increasing the values of the unsteadiness parameter decreases the velocity profile and this effect is associated with a reduction in the momentum boundary layer thickness in the velocity profile which illustrates that the unsteadiness parameter reduces the rate of flow due to stretching media. Fig 3 visualize the effects of the unsteadiness parameter (A) on the temperature profile and it was noticed that increasing the values of unsteadiness parameter decrease temperature. This can be justify physically because increasing the unsteadiness increases the rate of heat loss over stretching porous medium, thus causing in a decline in the temperature profile. Similar feature can be found in [16]. Fig 4 show the effects of Casson fluid parameter β on velocity

profile. The fluid velocity declines as the value of Casson fluid parameter is increasing and reduces the yield stress associated with fluid flow velocity Fig 5 establishes the effect of the thermal Grashof number on the velocity profiles. As the thermal Grashof number Gr has positive values these correspond to cooling of the porous medium. It is noted that an increase in the value of the thermal Grashof number leads to the rise in fluid velocity. This is because the buoyancy force improves the fluid velocity and increases the boundary layer thickness with an increase in the value of the thermal Grashof number. Fig 6 clarifies the effects of the magnetic parameter M on the velocity profiles. The velocity curve displays that the transport rates is reduced as the magnetic parameter values is increasing this is remarkably due to Lorentz force which is a drag force that acts to slow down fluid flow, hence raising the magnetic field parameter reduces flow velocity because it induces a Lorentz force that acts to slow down fluid flow, the outcome qualitatively agree with the anticipations, since the magnetic field exerts impeding effect on free convection flows. Fig 7 describes the magnetic parameter effects on temperature profiles. It shows that the temperature profiles increase as the magnetic parameter. Fig 8. The Eckert number represents the connection between the fluid low kinetic energy and enthalpy. It expresses the change of kinetic energy into internal energy by the work done against the viscous fluid stress. The positive Eckert number illustrates cooling of the medium, i.e., loss of the heat to the fluid from the plate. It is clear that an increase in the Eckert number causes a decrease in temperature profile. Fig 9: It is observed that fluid velocity distribution decreases with an increasing the values of Forchheimer number. The comparison results of the Skin friction coefficient of some existing literature: Sharidan *et al.* [24], Waini *et al.* [14], under some certain conditions and absence of nanoparticles i.e., $A=0.8, Gr=f_s=\mathrm{Re}\,x=Ec=Q=M=0, \varepsilon 1=\varepsilon 2=\varepsilon 3=\varepsilon 4=\varepsilon 5=1 \quad \beta \to Da \to \infty$ were tabulated on Table 3. Table 4 illustrated the behavior of Skin friction coefficient and Nusselt number for different parameters. Fig 10 illustrated the relationship between flow velocity $f'(\eta)$ and stretching rate (*Fw*) of the porous medium. The flow velocity decreases as the stretching rate is increasing. However, the temperature (θ) is increasing as the heat source parameter Q is increasing as shown in Fig 11.

Table 3: Comparison table for values of $-f''(0)$ obtained for $\beta \to Da \to \infty$, $A = 0.8, Gr = f_s = Re\,x = Ec = Q = M = 0, \varepsilon 1 = \varepsilon 2 = \varepsilon 3 = \varepsilon 4 = \varepsilon 5 = 1$

Pr	$-f''(0)$ [24]	$-f''(0)$ [14]	**Present work**
0.1	1.261042	1.2601097	1.26104260943067
1.0	1.261042	1.2601097	1.26104260943067
10.0	1.261042	1.2601097	1.26104260943067

Table 4: Skin friction coefficient and local Nusselt for different parameters

Rex	***A***	$-\left(1+\frac{1}{\beta}\right)f''(0)$	$-\theta'(0)$
0.01	0.0	1.17112992066557	1.48311764849605
0.01	0.8	1.23511682922678	0.993443007382589
0.01	1.0	1.25080840776565	0.867399188995573
0.1	0.0	1.21666765313502	1.46974175337887
0.1	0.8	1.27954425886941	0.978896222524280
0.1	1.0	1.29496798726371	0.852663180400173
1.0	0.0	1.63351265806513	1.33709355302921
1.0	0.8	1.68722097793645	0.836456149092115
1.0	1.0	1.70042971979946	0.708783952313546

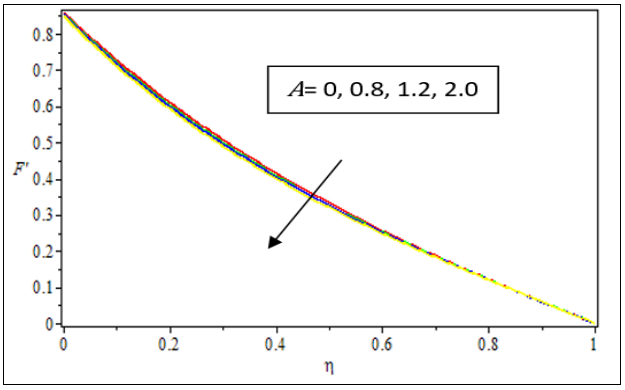

Fig 2: Behavior of f '(η) against *A*

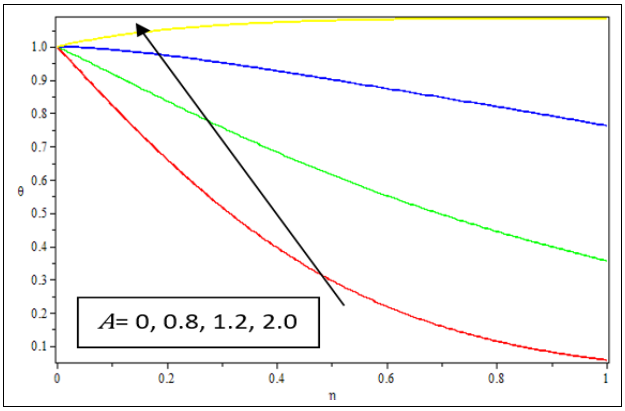

Fig 3: Behavior of θ(η) against *A*

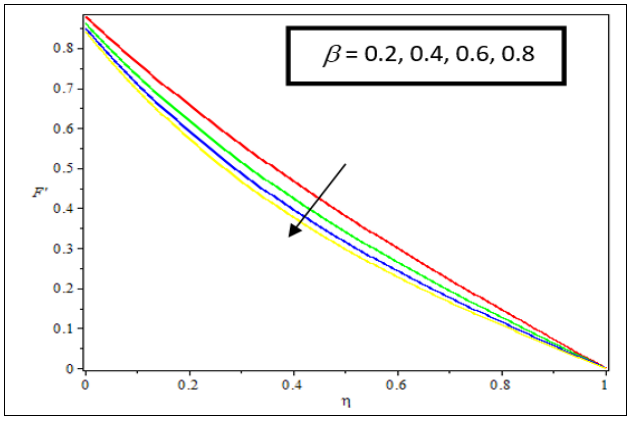

Fig 4: Behavior of f '(η) against *β*

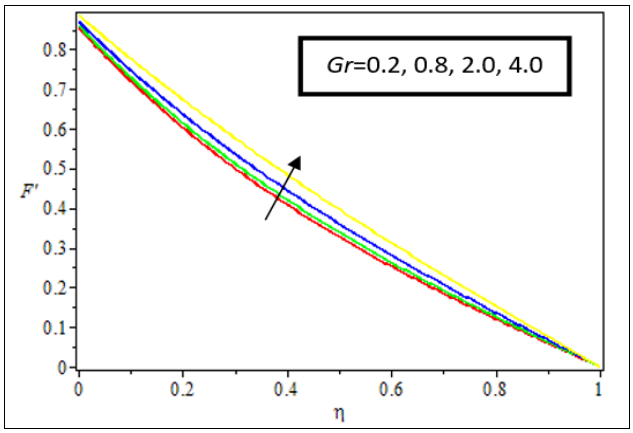

Fig 5: Behavior of f '(η) against *Gr*

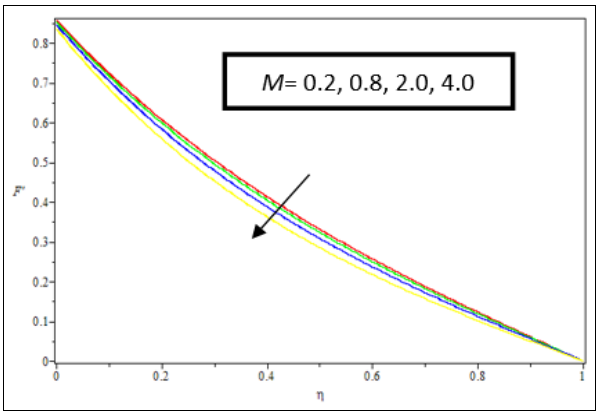

Fig 6: Behavior of f '(η) against *M*

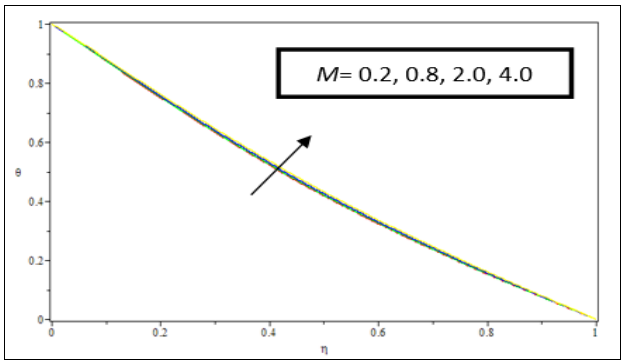

Fig 7: Behavior of θ(η) against *M*

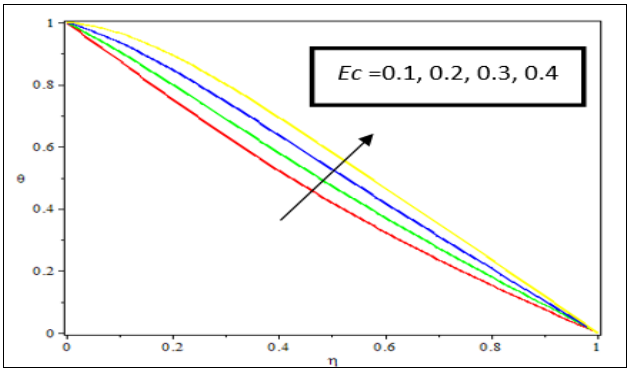

Fig 8: Behavior of θ(η) against *Ec*

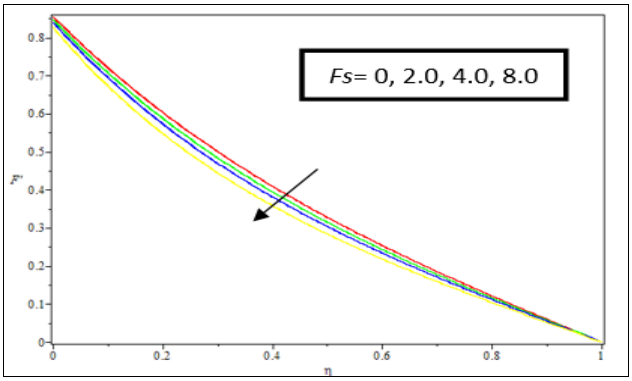

Fig 9: Behavior of f '(η) against *Fs*

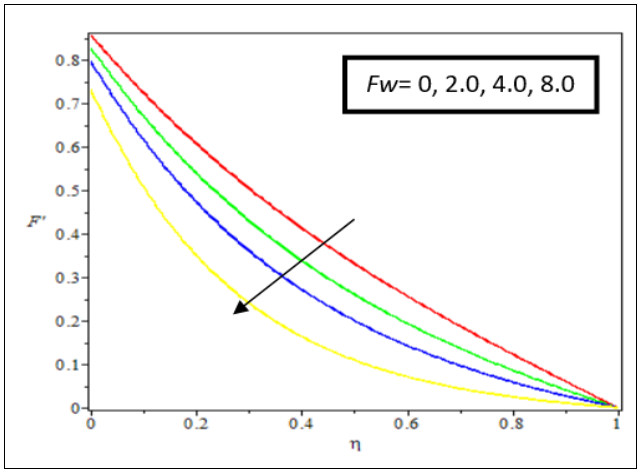

Fig 10: Behavior of f '(η) against *Fw*

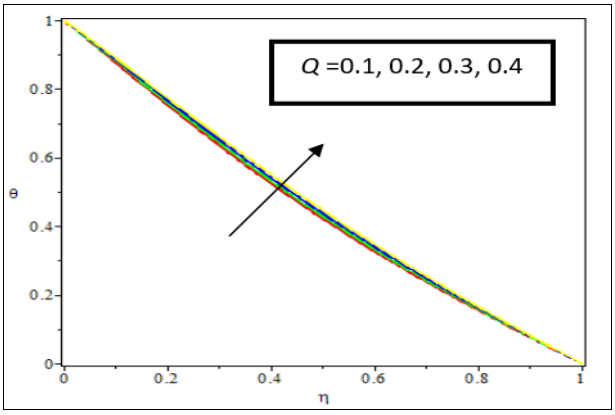

Fig 11: Behavior of θ(η) against Q

4. Conclusion

In this article, the effect of heat generation and MHD on unsteady Casson non-Newtonian hybrid nanofluid flow over stretching porous medium was studied theoretically. The PDEs were converted with the help of a similarity variable, and the resulting non-linear ODEs were solved using FDM with the help of the MAPLE 18.0 software. The influence of the following factors on the velocity and temperature profiles is taken into account. The following are the resulting conclusions:

1. The velocity profile decreases as the unsteadiness parameter increases.
2. The temperature profile is increased when the unsteadiness parameter is increased.
3. The velocity profile is reduced when the Casson fluid parameter increases.
4. The velocity profile raises increase in thermal Grashof number.
5. The temperature profile rises as Eckert number increase.
6. The velocity profile decreases with increase in the Forchheimer number.
7. The velocity decreases as stretching rate increases.
8. The temperature increase as the value heat source parameter increases.

Table 5: Nomenclature

u, v	Fluid velocity in x and y direction
t	time
ρ_{hnf}	Density of the hybrid nanofluid
ρ_{s1}	Density of the hybrid nanoparticles MoS_2
ρ_{s2}	Density of the hybrid nanoparticles SiO_2
μ_{hnf}	Dynamic viscosity of hybrid nanofluids
ν	Kinematic viscosity
c	Initial stretching rate
α	Constant of proportionality $(time)^{-1}$
B	Variable Magnetic field
B_0	Constant
cp	Specific heat capacity at constant volume
μ_f	Dynamic viscosity of the fluid
μ_B	Non-Newtonian fluid dynamic
β	Casson Parameter
B_o	Applied magnetic induction
g	Acceleration due to gravity
λ_T	Thermal expansion coefficient
λ_C	Mass expansion coefficient
T	Fluid temperature
T_∞	Free stream temperature
Q	Dimensional heat generation coefficient
σ_{nf}	Electrical conductivity of the Nanofluid
σ_{hnf}	Electrical conductivity of the Hybrid Nanofluid
σ_1	Electrical conductivity of the Hybrid Nanoparticle MoS
σ_2	Electrical conductivity of the Hybrid Nanoparticle SiO2
β_T	Thermal Expans Coefficient
u_w	Reference velocity
μ_{nf}	Dynamic viscosity of the nanofluids
μ_{hnf}	Dynamic viscosity of the hybrid nanofluids
μ_f	Dynamic viscosity of the fluid
$(\rho\beta)_{nf}$	Coefficient of the thermal expansion of the nanofluids

$(\rho\beta)_{hnf}$	Coefficient of the thermal expansion of the hybrid nanofluids
$(\rho\beta)_{s1}$	Coefficient of the thermal expansion of the MoS_2
$(\rho\beta)_{s2}$	Coefficient of the thermal expansion of the SiO_2
$(\rho\beta)_{f}$	Coefficient of the thermal expansion of the fluid
ν_{hnf}	Kinematic viscosity hybrid nanofluids
k_{hnf}	Thermal Conductivity of the hybrid nanofluids
k_{bf}	Electrical conductivity of the base fluid.
k_{s1}	Electrical conductivity of the MoS_2
k_{s2}	Electrical conductivity of the SiO_2
f	Velocity profile
η	Similarity variable
θ	Temperature profile
τ	Particles heat capacity to fluid heat capacity ratio
σ	Electrical conductivity of the surface temperature
T_w	Wall temperature
A	Unsteadiness Parameter
μ_∞	Constant viscosity
ψ	Stream function
M	Magnetic Parameter
F_s	Forchheimer parameter
Rex	Local Renold number
G_r	Thermal Grashof number
ϕ_1	The volume fraction of nanoparticle solid MoS_2
ϕ_2	The volume fraction of SiO_2
$(\rho cp)_{hnf}$	Specific heat capacity of hybrid nanofluid
$(\rho cp)_{s1}$	Specific heat capacity of MoS_2
$(\rho cp)_{s2}$	Specific heat capacity of SiO_2
E_c	Eckert number
P_r	Prandtl number
Nu	Nusselt number
Da	Darcy number
C_f	Skin Friction coefficient
π	Product of the rate of strain tensor with tensor, component of the deformation rate.
π_c	Critical value of the product based on the non-Newtonian model.
P_y	Fluid yield stress of the liquid
e_{ij}	Product of the rate of strain tensor with tensor.
I,j	Component of the deformation rate.

5. Acknowledgment
The authors acknowledge the Department of Pure and Applied Mathematics, Ladoke Akintola University of Technology's superb research facilities.

6. Conflict of Interests
There are no competing interests declared by the author(s).

7. References
1. Rashidi MM, Nazari MA, Mahariq I, Assad MEH, Ali ME, Almuzaiqer R, *et al*. Thermophysical properties of hybrid nanofluids and the proposed models: An updated comprehensive study. In Nanomaterials. MDPI. 2021; 11(11). Doi: https://doi.org/10.3390/nano11113084
2. Rehman A, Salleh Z, Mousa AAA, Bonyah E, Khan W. Analytical study of Time-Dependent MHD Casson Hybrid Nanofluid over a Stretchin Considering. Thermal Radiation. Advances in Mathematical Physics, 2022, 1-11.
3. Zaimi K, Ishak A, Pop I. Boundary layer flow and heat transfer past a permeable shrinking sheet in a nanofluid with radiation effect. Advances in Mechanical Engineering, 2012. Doi: https://doi.org/10.1155/2012/340354
4. Kamran A, Hussain S, Sagheer M, Akmal N. A numerical study of magnetohydrodynamics flow in Cassonnanofluid combined with Joule heating and slip boundary conditions. Results in Physics. 2017; 7:3037-3048. Doi: https://doi.org/10.1016/j.rinp.2017.08.004
5. Ogunsola AW, Akindele AO. Mixture of Al_2O_3-Cu/H_2O-$(CH_2OH)_2$ MHD hybrid nanofluid flow due to a stretchable rotating disks system under the influence of non-uniform heat source or sink and thermal radiation. J. Math. Comput. Sci. 2022; 12:p8. ISSN: 1927-5307. Doi: https://doi.org/10.28919/jmcs/6624
6. Makinde DO, Abdul Aziz. Boundary layer flow of a nanofluid past a stretching sheet with a convective boundary condition. International Journal of Thermal Sciences. 2011; 50(7):p1326. https://www.sciencedirect.com/science/article/abs/pii/S1290072911000603?via%3Dihub

7. Ghadikolaei SS, Yassari M, Sadeghi, Dawood D. GInvestigation on thermophysical proper ties of Tio 2 -Cu/H 2 O hybrid nanofluid transport dependent on shape factor in MHD stagnation point flow Powder Technology. 2017; 322(1). 10.1016/j.powtec.2017.09.006Project: Non- Newtoniananofluid flow.
8. Omar NS, Bachok N, Arifin N. Md. Stagnation Point Flow Over a Stretching or Shrinking Cylinder in a Copper-Water Nanofluid. Indian Journal of Science and Technology. 2015; 8(31). Doi: https://doi.org/10.17485/ijst/2015/v8i31/85405
9. Tayebi T, Chamkha AJ. Free convection enhancement in an annulus between horizontal confocal elliptical cylinders using hybrid nanofluids. Numerical Heat Transfer; Part A: Applications. 2016; 70(10):1141-1156. Doi: https://doi.org/10.1080/10407782.2016.1230423
10. Kamel MS, Al-Oran O, Lezsovits F. Thermal conductivity of Al_2 O_3 and CeO_2 nanoparticles and their hybrid based water nanofluids: An experimental study. PeriodicaPolytechnica Chemical Engineering. 2020; 65(1):50-60. Doi: https://doi.org/10.3311/PPch.15382
11. Lund LA, Omar Z, Khan I, Raza J, Sherif ESM, Seikh AH. Magnetohydrodynamic (MHD) flow of micropolar fluid with effects of viscous dissipation and joule heating over an exponential shrinking sheet: Triple solutions and stability analysis. Symmetry. 2020; 12(1). Doi: https://doi.org/10.3390/sym12010142
12. Mjankwi MA, Masanja VG, Mureithi EW, James MNO. Unsteady MHD Flow of Nanofluid with Variable Properties over a Stretching Sheet in the Presence of Thermal Radiation and Chemical Reaction. International Journal of Mathematics and Mathematical Sciences, 2019. Doi: https://doi.org/10.1155/2019/7392459
13. Sobamowo MG, Akinshilo AT, Yinusa AA. Thermo-Magneto-Solutal Squeezing Flow of Nanofluid between Two Parallel Disks Embedded in a Porous Medium: Effects of Nanoparticle Geometry, Slip and Temperature Jump Conditions. Modelling and Simulation in Engineering, 2018. Doi: https://doi.org/10.1155/2018/7364634
14. Waini I, Amira Zainal N, Safwa Khashi N, Basyaruddin Abdul Rahman M, Rahman MohdKasim A, Farahain Mohammad N. Numerical study of unsteady Casson fluid flow and heat transfer over a stretching surface with modified magnetic field effects, 2018. https://www.researchgate.net/publication/341149313
15. Goud Bejawada S, Dharmendar Reddy Y, Jamshed W, Nisar KS, Alharbi AN, Chouikh R. Radiation effect on MHD Casson fluid flow over an inclined non-linear surface with chemical reaction in a Forchheimer porous medium: Radiation effect on MHD Casson fluid flow over an inclined non-linear surface. Alexandria Engineering Journal. 2022; 61(10):8207-8220. Doi: https://doi.org/10.1016/j.aej.2022.01.04
16. Mukhopadhyay S, De PR, Bhattacharyya K, Layek GC. Casson fluid flow over an unsteady stretching surface. Ain Shams Engineering Journal. 2013; 4(4):933-938. Doi: https://doi.org/10.1016/j.asej.2013.04.004
17. Akindele AO, Ogunsola AW. A study of non-isothermal permeable flow of nano-fluid in a stretchable rotating disk system. J. Math. Comput. Sci. 2021; 11(2):1486-1498. ISSN: 1927-5307.
18. Obalalu AM, Ajala OA, Abdulraheem A, Akindele AO. The influence of variable electrical conductivity on non-DarcianCassonnanofluid flow with first and second-order slip conditions. Partial Differential Equations in Applied Mathematics. 2021; 4:p100084.
19. Obalalu AM, Ajala AO, Akindele AO, Oladapo OA, Adepoju O, Jimoh OM. Unsteady squeezed flow and heat transfer of dissipative casson fluid using optimalhomotopy analysis method: An application of solar radiation. Partial Diff EquApplMath, 2021, p100146. Doi: http://dx.doi.org/10.1016/j.padiff.2021.100146
20. Akindele AO, Ogunsola AW, Obalalu AM, Adegbite P, Ajala OA, Alao S. Mhd flow of nano-fluid with non-uniform heat source or sink in the presence of chemical reaction and activation energy. Journal of Advance Research in Applied Science. 2021; 8(5). ISSN: 2208-2352
21. Obalalu AM, Ajala OA, Akindele AO, Alao S, Adepoju O. Effect of melting heat transfer on electro magnet ohydrodynamic non-newtoniannanofluid flow over a riga plate with chemical reactionand arrhenius activation energy. Eur. Phys. J. Plus. 2021; 136:p891.Doi: https://doi.org/10.1140/epjp/s13360-021-01869-z
22. Obalalu AM, Ajala OA, Adeosun TA, Akindele AO, Oladapo OA, Olajide OA, Adegbite P. Significance of variable electrical conductivity on non-Newtonian fluid flowbetween two vertical plates in the coexistence of Arrhenius energy andexothermic chemical reaction.Partial Diff EquApplMath, 2021. Doi: https://doi.org/10.1016/j.padiff.2021.100184\
23. Akindele AO, Ajala OA, Adegbite P, Ogunsola AW. Convective Flow of Nanofluids Using Blasius-Rayleigh-Stoke Variable with Slip Effect, IOSR Journal of Mathematics. (IOSR-JM) e-ISSN: 2278-5728. 2021; 17(3):1-8. p-ISSN: 2319-765X.
24. Sharidan S, Mahmood T, Pop I. Similarity solutions for the unsteady boundary layer flow and heat transfer due to a stretching sheet. International Journal of Applied Mechanics and Engineering. 2006; 11(3):647-654.